

# Generation and manipulation of bright spatial bound-soliton pairs under the diffusion effect in photovoltaic photorefractive crystals\*

Ze-Xian Zhang(张泽贤), Xiao-Yang Zhao(赵晓阳), Ye Li(李烨), Hu Cui(崔虎)<sup>†</sup>,  
Zhi-Chao Luo(罗智超), Wen-Cheng Xu(徐文成), and Ai-Ping Luo(罗爱平)

Guangdong Provincial Key Laboratory of Nanophotonic Functional Materials and Devices & Guangzhou Key Laboratory for Special Fiber Photonic Devices and Applications, South China Normal University, Guangzhou 510006, China

(Received 12 May 2020; revised manuscript received 15 June 2020; accepted manuscript online 1 August 2020)

The generation and propagation characteristics of bright spatial bound-soliton pairs (BSPs) are investigated under the diffusion effect in photovoltaic photorefractive crystals by numerical simulation. The results show that two coherent solitons, one as the signal light and the other as the control light, can form a BSP when the peak intensity of the control light is appropriately selected. Moreover, under the diffusion effect, the BSP experiences a self-bending process during propagating and the center of the BSP moves on a parabolic trajectory. Furthermore, the lateral shift of the BSP at the output face of the crystal can be manipulated by adjusting the peak intensity of the control light. The research results provide a method for the design of all-optical switching and routing based on the manipulation of the lateral position of BSPs.

**Keywords:** solitons, photovoltaic photorefractive, diffusion effect

**PACS:** 42.65.Tg, 42.65.-k

**DOI:** 10.1088/1674-1056/abab7a

## 1. Introduction

The interactions between optical solitons have always been attracting attention in the field of nonlinear optics since the interactions present lots of novel and fascinating phenomena such as soliton fusion, fission, and annihilation, as well as spiraling.<sup>[1–8]</sup> Wang *et al.* investigated numerically the propagation and interactions of Airy–Gaussian beams in a cubic–quintic nonlinear medium, and found that soliton pairs can be obtained by adjusting the phase shift and interval between two Airy–Gaussian beams.<sup>[9]</sup> Lan *et al.* proposed a general propagation lattice Boltzmann model for a variable-coefficient compound Korteweg–de Vries–Burgers equation by selecting an equilibrium distribution function and adding a compensation function, and simulated the two-soliton solution by taking appropriate free parameters.<sup>[10]</sup> Lan *et al.* also investigated a non-autonomous generalized AB system, and found that the two short waves and mean flow can appear as the solitary waves.<sup>[11]</sup> These various phenomena undoubtedly illustrate that optical solitons are excellent candidates to realize all-optical switching and routing,<sup>[12–15]</sup> which are key technologies for all-optical communication network based on light controlling light. Until now, optical solitons have been studied, which can exist in many kinds of nonlinear optical materials such as Kerr medium,<sup>[16,17]</sup> photorefractive (PR) crystal,<sup>[18–21]</sup> and liquid crystal.<sup>[22,23]</sup> In the recent decade, researches on PR solitons in PR crystals are of great realistic significance, because only extremely low light intensities are needed to form PR solitons, meanwhile, a weak PR soliton beam can be acted

as the control beam to induce an optical waveguide, guiding a strong non-soliton beam acting as the signal beam.<sup>[24,25]</sup>

Many studies on PR solitons show that the diffusion effect in PR crystals introduces an asymmetric tilt in the light-induced PR waveguide, therefore exhibiting an effect on the propagation trajectory of the PR solitons.<sup>[26,27]</sup> Moreover, when two PR solitons propagate in a PR crystal simultaneously, the diffusion effect has a significant effect on both their propagation trajectories and the interactions between them.<sup>[28]</sup> Furthermore, it has been widely reported that the diffusion effect depends on the width of PR spatial solitons, the narrower width of a PR spatial soliton results in a stronger diffusion effect exerting on the PR spatial soliton. At present, the studies on the diffusion effect are of great practical significance for the design and fabrication of micro-nano all-optical devices based on PR crystals, because both the width of optical signals and the dimension of optical devices are becoming smaller with the development of the manufacturing technology of integrated optical components. Some studies have shown that the diffusion effect is not beneficial for the stable propagation of PR solitons, which also provide some methods to suppress adverse effects arising from the diffusion effect.<sup>[26,29–31]</sup> However, in some cases, the diffusion effect may become advantageous for manipulating the propagation behaviors of PR solitons. In this paper, our studies show that two coherent solitons, one as the signal light and the other as the control light, can form a bound-soliton pair (BSP) by appropriately selecting the peak intensity of the control light under the diffusion effect in a photovoltaic (PV) PR crystal, the BSP as a whole

\*Project supported by the National Natural Science Foundation of China (Grant Nos. 61875058, 11874018, 11974006, and 61378036).

<sup>†</sup>Corresponding author. E-mail: cuihu@m.scnu.edu.cn

experiences a self-bending process and the propagation trajectory (the lateral shift) of the BSP in (at the output face of) the crystal can be manipulated by adjusting the peak intensity of the control light. Our studies demonstrate that the designed all-optical switching and routing can be implemented based on the manipulation of the lateral position of BSPs through making full use of the advantages of the diffusion effect.

This paper is organized as follows. In Section 2, we introduce the theory and method. Section 3 presents extraordinary optical phenomenon and analysis. Finally, Section 4 presents the summary of this paper.

## 2. Theory and method

### 2.1. One-soliton model

To investigate the interactions between two coherent solitons, we first consider the case that a single signal beam launched into a PV PR crystal propagates along the  $z$ -axis, which is allowed to diffract only along the  $x$ -direction. A uniform background beam, which propagates along the same direction with the signal beam, is introduced to illuminate the whole PV PR crystal and promote the signal beam to form a PV PR soliton. The PV PR crystal in our study is selected to be copper-doped  $\text{K}_{0.25}\text{Na}_{0.75}\text{Sr}_{1.5}\text{Ba}_{0.5}\text{Nb}_{0.5}\text{O}_{15}$  (Cu:KNSBN) and the crystalline  $c$ -axis is oriented along the  $x$  coordinate. Furthermore, we assume that the signal beam and the uniform background beam are an e ray and an o ray, respectively. For the case assuming no loss of crystal, the propagation of the signal beam in a PV PR crystal under the open-circuit condition is described by the following normalized equation:<sup>[32]</sup>

$$i \frac{\partial u}{\partial \zeta} = -\frac{1}{2} \frac{\partial^2 u}{\partial \xi^2} - \beta \frac{1+r|u|^2}{1+|u|^2} u - \gamma \frac{\partial \ln(1+|u|^2)}{\partial \xi} u. \quad (1)$$

In this equation,  $u$  is the normalized slowly varying envelope of the signal beam and  $|u|^2 = s_e I_e / (s_o I_o)$ , where  $s_e$  and  $s_o$  ( $I_e$  and  $I_o$ ) are the photoionization cross sections (the intensities) of the e ray and the o ray, respectively.  $\xi = x/x_0$  denotes the normalized transverse coordinate and  $x_0$  is an arbitrary spatial scale.  $\zeta = z/(k_e x_0^2)$  is the normalized propagation distance and the wave number of the e ray is given by  $k_e = 2\pi n_e / \lambda_e$ , where  $n_e$  is the unperturbed extraordinary index of refraction and  $\lambda_e$  is the free-space wavelength of the e ray.  $r = \kappa^e / \kappa^o$ , where  $\kappa^e$  and  $\kappa^o$  are the Glass constants of the e ray and the o ray, respectively.  $\beta = n_e^2 k_e^2 x_0^2 r_{\text{eff}} E_{\text{pv}} / 2$  is associated with the drift effect and  $\gamma = n_e^2 k_e^2 x_0 r_{\text{eff}} K_B T / (2q)$  is related to the diffusion effect, where  $r_{\text{eff}}$ ,  $K_B$ ,  $T$  and  $q$  are the effective electro-optic coefficient, Boltzmann's constant, the absolute temperature, and the carrier charge, respectively.  $E_{\text{pv}} = k^o \gamma_R N_A / (q\mu)$  is the PV field, where  $k^o$ ,  $\gamma_R$ ,  $N_A$ , and  $\mu$  represent the PV coefficient of the o ray, the carrier recombination rate, the density

of the acceptor, and the mobility of the charge carrier, respectively.

To search for soliton solutions of Eq. (1), the diffusion term of Eq. (1) can be neglected because soliton beams can be only induced by the diffusion term to deflect, exhibiting no effect on the intensity profile of soliton beams. Supposing  $\gamma = 0$ , equation (1) is simplified to a nonlinear Schrödinger equation with a higher-order nonlinearity. We search for stationary solutions of Eq. (1) in the following form:

$$u(\xi, \zeta) = y(\xi) \exp(i\Gamma \zeta), \quad (2)$$

where  $\Gamma$  represents a nonlinear shift of the propagation constant. Substituting Eq. (2) into Eq. (1) (with  $\gamma = 0$ ), the PV PR soliton equation is obtained as follows:

$$\frac{d^2 y}{d\xi^2} = 2 \left[ \Gamma - \beta \frac{1+r|y|^2}{1+|y|^2} \right] y. \quad (3)$$

We express  $y$  in the usual fashion  $y(\xi) = A^{1/2} \eta(\xi)$ , where the positive quantity  $A$  is the peak intensity of the soliton solutions and  $\eta(\xi)$  denotes a normalized real function bounded by  $0 \leq \eta(\xi) \leq 1$ . By substituting this form of  $y$  into Eq. (3) and employing the boundary conditions  $\eta(\xi \rightarrow \pm\infty) = 0$ ,  $\eta(0) = 1$  as well as  $\eta'(0) = 0$ , we find that

$$\Gamma = \beta r - \beta \frac{r-1}{A} \ln(1+A), \quad (4)$$

$$\eta'' = \frac{2\beta(r-1)}{A} [\ln(1+A\eta^2) - \eta^2 \ln(1+A)]. \quad (5)$$

The functional form  $\eta(\xi)$  for bright soliton solutions can be obtained by numerically integrating Eq. (5) when  $\beta > 0$  and  $r > 1$ . In our numerical integration, the arbitrary spatial scale  $x_0$  is selected to be  $8 \mu\text{m}$  and the free-space wavelength  $\lambda_e$  is determined to be  $488 \text{ nm}$ . For Cu:KNSBN crystals, the following parameters are employed:  $n_e = 2.25$ ,  $r = 2.5$ ,  $r_{\text{eff}} = 820 \text{ pm/V}$ , and  $E_{\text{pv}} = 20 \text{ kV/cm}$ .<sup>[33,34]</sup> The existence curve of bright soliton solutions of Eq. (5) is shown in Fig. 1. It can be noted that the full width at half maximum (FWHM) of the intensity of the soliton beams decreases with the increase of  $A$  when  $A < 2$ . The important thing to note here is that the existence curve is an oblique straight line approximation and its slope is approximately equal to  $-1$  when  $0.1 \leq A \leq 0.3$ .

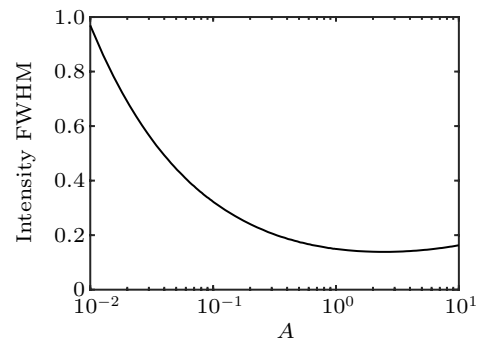


Fig. 1. Intensity FWHM of bright solitons versus  $A$ .

### 2.2. Two-soliton model

The coherent superposition state of two soliton beams at the input face of the crystal in the general form is given as

$$u(\xi, 0) = A_1^{1/2} \eta_1 \left( \xi + \frac{h_0}{2} \right) + A_2^{1/2} \eta_2 \left( \xi - \frac{h_0}{2} \right) \exp(i\theta). \quad (6)$$

In this equation,  $A_1$  and  $A_2$  are the initial peak intensities of the first and the second solitons, respectively;  $\eta_1(\xi)$  and  $\eta_2(\xi)$  represent the initial normalized intensity profiles of the first and the second solitons, respectively;  $h_0$  and  $\theta$  are the initial separation and phase difference between the two solitons, respectively. In our numerical simulation, the initial separation  $h_0$  is determined to be 0.9, which can make sure that the two solitons are close enough and their edges overlap, namely, two solitons can affect each other. Substituting Eq. (6) into Eq. (1), we can investigate the dynamics evolution process of two coherent solitons under the diffusion effect by numerically solving Eq. (1) with the beam propagation method. We select  $T = 284$  K and find that  $\gamma$  in Eq. (1) is equal to 0.341.

### 2.3. Variance $D$ of the separation between two solitons

The dynamic stability of two coherent solitons under the diffusion effect can be investigated by analyzing the variance of the separation between the two coherent solitons propagating through the entire length of the crystal. The variance  $D$  of the separation between two solitons is calculated as follows:

$$D = \frac{1}{L} \int_0^L (h(\zeta) - \bar{h})^2 d\zeta, \quad (7)$$

where  $L$  is the normalized length of the crystal,  $h(\zeta)$  denotes the separation between the two solitons, and the mean value  $\bar{h}$  of  $h(\zeta)$  is given by  $\bar{h} = \int_0^L h(\zeta) d\zeta / L$ . In our numerical simulation, we first use the split-step Fourier transform method to solve Eq. (1) numerically; then on the base of this, we use numerical calculation to obtain the numerical value of  $h(\zeta)$ . When the variance  $D$  is extremely small, the two solitons bound together and form a BSP. Moreover, the smaller the variance  $D$  is, the more stable the BSP becomes.

To search for BSPs, the variance  $D$  is calculated by varying  $A_2$  and fixing  $A_1$  at 0.1. The solid curve in Fig. 2 shows the correspondence relation between  $D$  and  $A_2$  for two incident solitons with opposite phase ( $\theta = \pi$ ). It should be noted that there are three larger basins with a flat bottom, which are centered at about  $A_2 = 0.176, 0.231,$  and  $0.258$ , respectively. The BSPs composed of two anti-phase solitons exist in the three basins, because the variance  $D$  is approximately equal to 0 in the three basins (see the solid curve in Fig. 2(b)). The reasons for this judgment criterion are as follows. When two interacting solitons are stable and form a BSP, the separation  $h(\zeta)$  between the two solitons is approximately constant and equal

to the initial separation  $h_0$ ; moreover, the mean value  $\bar{h}$  of  $h(\zeta)$  is approximately equal to the initial separation  $h_0$ . Therefore, the variance  $D$  calculated by Eq. (7) is approximately equal to 0 for two stable interacting solitons. Furthermore, the BSPs are robust against the light intensity perturbation due to a large width of the three basins, which implies that the small fluctuation of  $A_2$  is allowed. This is very important for the consecutive stability of BSPs upon formation because the output power of lasers is fluctuating due to time aging in practice. So, the three basins can be regarded as stable regions of BSPs. In addition, the dashed curve in Fig. 2 shows the correspondence relation between  $D$  and  $A_2$  for two incident solitons with the same phase ( $\theta = 0$ ). It can be found by comparing the two curves in Fig. 2 that the varying trend of the dashed curve is similar to that of the solid curve, meanwhile the dashed curve also shows three larger basins, namely, three stable regions are centered at about  $A_2 = 0.139, 0.196,$  and  $0.253$ , respectively.

It should be pointed out that there is no stable region for BSPs when  $A_2$  is much larger than  $A_1$ , due to the weak interference effect between two solitons under the large amplitude difference of the two solitons. Moreover, the unstable as well as stable regions alternate with each other and the widths of the three stable regions decrease in turn, this results from that the interference effect between two solitons shows oscillating attenuation with the increased amplitude difference of the two solitons.

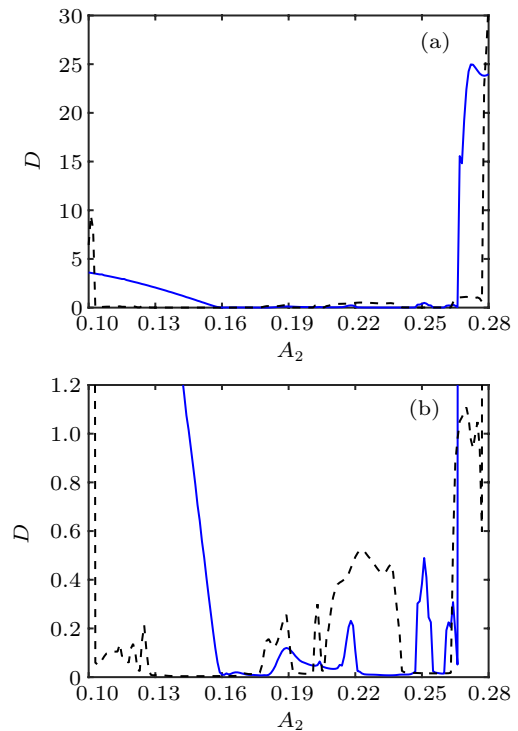


Fig. 2. (a) Sum of squares of deviations from mean  $D$  as a function of  $A_2$  for the cases of  $\theta = \pi$  (solid curve) and  $\theta = 0$  (dashed curve). Panel (b) is enlargement of (a) in the vertical direction.

### 3. Extraordinary optical phenomenon and analysis

#### 3.1. Propagation dynamics of two anti-phase solitons

The propagation dynamics of two coherent interacting solitons is simulated numerically as follows. When two out of phase solitons are launched, the trajectories of the two solitons are shown in Fig. 3 in the  $\xi$ - $\zeta$  plane by plotting the intensity contours for  $A_1 = 0.1$  and several values of  $A_2$ . The left soli-

ton and the right soliton are regarded as the signal light and the control light, respectively.

The magnitude of the diffusion effect received can be changed by changing the amplitude of the right soliton, because the diffusion effect depends on the width of PR spatial solitons, and that the narrower width of a PR spatial soliton contributes to the stronger diffusion effect exerting on the PR spatial soliton.

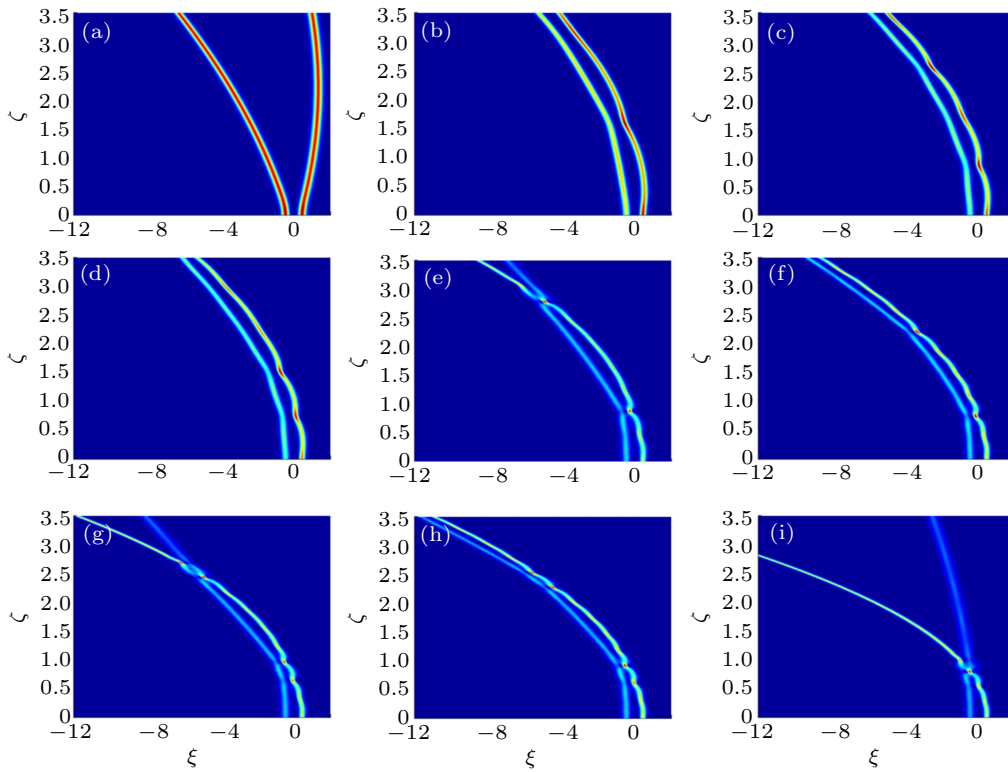


**Fig. 3.** Intensity contours showing the propagation dynamics of two out of phase solitons for  $A_1 = 0.1$  and  $A_2 = 0.1$  (a), 0.163 (b), 0.176 (c), 0.181 (d), 0.214 (e), 0.231 (f), 0.251 (g), 0.258 (h), 0.28 (i).

The results show that they will be repelled and separated from each other under the same amplitudes of the two solitons, and the distance between the two solitons will increase with the increased propagation distance (see Fig. 3(a)). When  $A_2$  is in the first stable region, the control light and signal light show periodic attraction and repulsion with the increased amplitudes of the control light, afterwards, the two beams interact repeatedly. And the positions of the two beam exit surfaces increase with the increased intensity of the control light (see Figs. 3(b)–3(d)). Once  $A_2$  reaches the unstable region, the two beams will produce a similar collision effect, leading to no soliton pair. The control light and signal light show mutual attraction and collide after propagating for a short distance. There is a strong energy exchange during this period. The energy is transferred from the signal light to the control light, resulting in the separated two beams (see Figs. 3(e), 3(g), and 3(i)). Similarly, when  $A_2$  is in the second and the third stable regions, the distance between the two beams will be slightly reduced, but the two beams still show periodic attraction and

repulsion for a certain transmission distance, contributing to a stable pair of solitons.

For the interaction of the above two beams, we understand that the self-focusing effect will occur when the soliton is produced in the crystal, which will lead to the change of its background refractive index discovery, finally the behavior between the two beams is influenced. The two solitons have destructive interference in the overlapped region under the equal amplitudes of the two beams due to phase difference, and the background refractive index of the overlapped region decreases, resulting in a repulsive effect between the two solitons. When the amplitude of the control light changes, it has been shown that BSPs will be formed, exhibiting periodic attraction and repulsion when the amplitude difference of the two opposite beams is not too large.<sup>[35]</sup> A similar "collision effect" occurs under the large amplitude difference. Therefore, the diffusion effect has two functions, one of which is the balance of two beams to form a stable pair of solitons. The results also explain the stable region, which is the result

of the balance between the diffusion effect and the interaction of unequal amplitude solitons. In the stable region, the interaction between the diffusion effect and the soliton is in equilibrium, however the two are not in the unstable region. Due to the existence of stable regions, such as  $[0.163, 0.181]$ ,  $[0.221, 0.247]$ , and  $[0.255, 0.260]$ , BSPs can also be formed when the amplitude  $A$  of the incident light fluctuates in the above-mentioned stable regions. Another function is to bend the beam. The narrower the beam is, the stronger the diffusion effect becomes, meanwhile the FWHM of the beam is inversely related to the beam amplitude  $A$ . Therefore, when the controlling optical amplitude  $A_2$  increases, the diffusion effect and the self-bending degree of the soliton pair both increase, which leads to the changed position of the soliton pair on the exit surface. It should be noted that the exit positions include but are not limited to these mentioned positions, and the amplitudes of the signal light and control light can be changed to make the exit surface position as satisfying as possible. By this means, we can construct a one-to-three all-optical switching device.

### 3.2. Relation between two anti-phase solitons

In order to investigate the relation between two solitons more intuitively, three most stable  $A_2$  values are selected in anti-phase relations of solitons to plot the relation graph of the spacing and propagation distance  $\xi$  between two solitons and the relation graph of the peak intensity and propagation distance  $\xi$  of two solitons (see Fig. 4).

The separation between the two solitons changes periodically with the increased distance (see Fig. 4(a)). Surprisingly, it is a strictly periodic relationship for  $A_2 = 0.176$ . Using the equivalent field, we can clearly know that the composite acceleration of the control light is oriented to the right at the beginning, and the acceleration from the repulsion between solitons decreases with the increased soliton interval, the final acceleration provided by the diffusion effect is greater than that of the repulsion. In simple terms, the control light is accelerated and then decelerated until zero of the final speed, then accelerated to the left. It should be emphasized that when the control light makes the above motion, the signal light is moving to the left at the same time, so the combined acceleration is still to the left when the control light returns to the initial position. Therefore, the peak of the interval will be closer than the peak when the solitons are close to each other under the separation from each other. For  $A_2 = 0.231$  and  $0.258$ , the equilibrium between soliton repulsion and diffusion effect fluctuates due to the significant enhancement of the diffusion effect. But it can be noted in the graph that the change is still approximately periodic even though some fluctuations occur, in addition, we can see from the maximum or the minimum that the soliton

spacing is not getting smaller and smaller but it is jittering in a small range.

Solitons generally exchange energy during their interactions. The peak intensity of the control light and the peak intensity of the signal light change periodically with the propagation distance, the peak intensity of the control light decreases first at the beginning, while the signal light increases first (see Fig. 4(b)). For  $A_2 = 0.176$ , the background refractive index between the two lights is inclined to the control light due to the greater amplitude of the control light than that of the signal light, as a result, the beam energy can be qualitatively understood as the transfer from the signal light to the control light. At the beginning, soliton pairs are separated due to anti-phase and repulsion. The larger soliton interval leads to the smaller inclination of the background refractive index. Therefore, the peak intensity of the control light decreases while the peak intensity of the signal light increases. Moreover, the peak intensity of the control light reaches the minimum value and the peak intensity of the signal light reaches the maximum value under the largest soliton interval. When the soliton interval is the smallest, the peak intensity of the control light reaches the maximum value and the peak intensity of the signal light reaches the minimum value. For  $A_2 = 0.231$  and  $0.258$ , the variation of peak intensity fluctuates and a number of submaximal values appear due to the significantly enhanced diffusion effect of the control light.

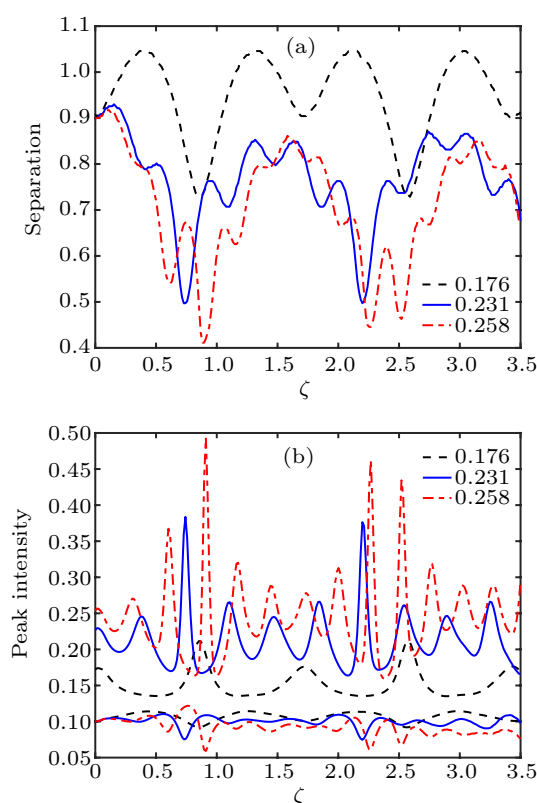
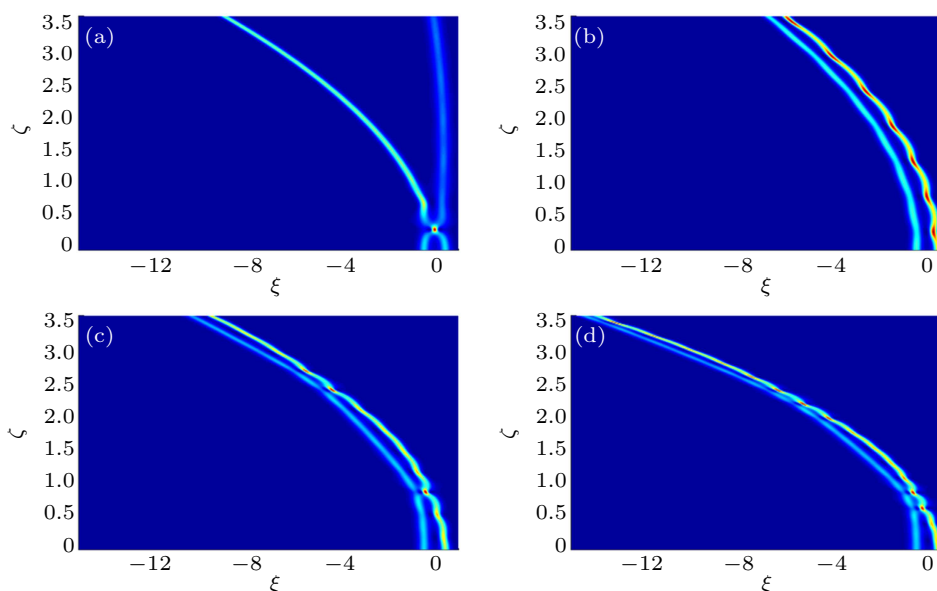


Fig. 4. Relation (a) between propagation distance  $\xi$  and the spacing, and (b) between  $\xi$  and the peak intensity for two anti-phase solitons.

### 3.3. Propagation dynamics of two in-phase solitons

Only considering  $A_2$  is in the stable region when two solitons are in the same phase, the motion trajectory of BSPs is shown in Fig. 5. The two solitons merge with each other after propagating for a short distance under the condition of same amplitudes of the control light and the signal light. With the strong energy exchange, the energy is transferred from the

signal light to the control light, leading to the separated two solitons. In the stable region, the bending degree of BSPs increases with the increased  $A_2$  as shown in Figs. 5(b)–5(d). It can be found that the transmission characteristics of BSPs formed by two in-phase solitons are similar to those of BSPs formed by two out of phase solitons, and that the in-phase solitons are more affected by the diffusion effect than the anti-phase solitons.



**Fig. 5.** Intensity contours showing the propagation dynamics of two in-phase solitons for  $A_1 = 0.1$  and  $A_2 = 0.1$  (a), 0.139 (b), 0.196 (c), and 0.253 (d).

### 3.4. Relation between two in-phase solitons

Three most stable  $A_2$  values in-phase relations of solitons are selected to plot the relation graph of the spacing and propagation distance  $\xi$  between two solitons and the relation graph of the peak intensity and propagation distance  $\xi$  of two solitons (see Fig. 6).

The periodic three cases decrease first as shown in Fig. 6(a). In particular, it is strictly periodic for  $A_2 = 0.139$ . It has been shown that the interactions among solitons with the same phase and unequal amplitude are still periodic in attracting separation without destroying the solitons themselves. The diffusion effect results in the increased distance between the attraction and the separation. Therefore, the control light is close to the signal light due to the in-phase attraction and diffusion effect in the initial state, then the two beams become separated arising from similar "elastic collision", thus forming a dynamic equilibrium. For  $A_2 = 0.196$  and 0.253, similar to the anti-phase case, it is also due to the enhanced diffusion effect that the equilibrium between the repulsion and the diffusion effect fluctuates. In particular, when  $A_2 = 0.253$ , it can be noted that the two solitons interval is slowly approaching, but it can still be regarded as a BSP at a given transmission distance.

The peak intensities of the control light and signal light

also vary periodically with the propagation distance (see Fig. 6(b)). The peak intensity of the signal light increases at the beginning, while the peak intensity of the signal light decreases first. And the changed principle of the three cases is similar to that of the anti-phase case. It is interesting to mention that the peak intensity is inversely proportional to the width of the soliton, as a result, the slightly changed width of the two beams periodically is achieved during the propagation process.

Although the mechanism of interaction between two coherent solitons is complicated, the formation process of BSP can be simply understood as follows. The relative phase difference between two solitons leads to varied refractive index in the overlap region, affecting the soliton interaction. Additionally, the diffusion process introduces an asymmetric tilt in the light-induced PR waveguide which will also influence the soliton interaction. Under the appropriate conditions, the co-effect of the relative phase difference and the diffusion results in the formation of BSPs. In particular, these two different effects are both associated with  $A_2$ , thus the appropriate choice of  $A_2$  contributes to the formation of BSPs.

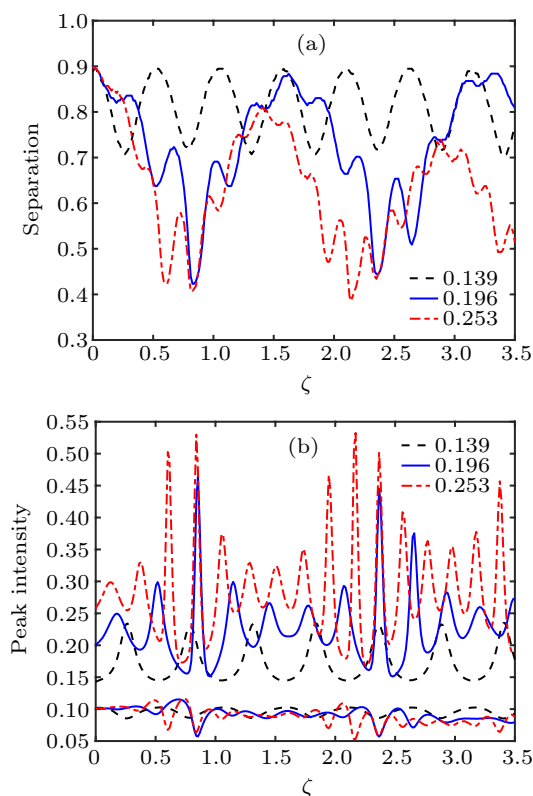


**Fig. 6.** Relation (a) between propagation distance  $\xi$  and the spacing, and (b) between  $\xi$  and the peak intensity for two in-phase solitons.

#### 4. Conclusion

The interaction between two bright solitons in PV PR crystals with diffusion effects is investigated by numerical simulations. These simulations show that a BSP can be formed by two solitons including the signal light and the control light when the peak intensity of the control light is appropriately selected. BSPs experience a self-bending process along a parabolic trajectory and the bending angle of BSPs depends strongly on the peak intensity of the control light. It is also found that the propagation characteristics of BSPs formed by two in phase solitons are similar to those of BSPs formed by two out of phase solitons. In addition, our results clearly demonstrate that a one-to-three all-optical switching device can be obtained by using the shift of the BSP positions at the crystal output face, also, the bending angle of BSPs can be controlled by adjusting the peak intensity of the control light. High precision surgical operations can be achieved in the medical field. This device also has potential applications in many

fields including optical signal processing and telecommunications.

#### References

- [1] Weerasekara G and Maruta A 2017 *IEEE Photon. J.* **9** 7903612
- [2] Wang Y F, Tian B and Jiang Y 2017 *Appl. Math. Comput.* **292** 448
- [3] Zhao X H, Tian B, Chai J, Wu X Y and Guo Y J 2017 *Eur. Phys. J. Plus* **132** 192
- [4] Kudlinski A, Wang S F, Mussot A and Conforti M 2015 *Opt. Lett.* **40** 2142
- [5] Yang C Y, Li W Y, Yu W T, Liu M L, Zhang Y J, Ma G L, Lei M and Liu W J 2018 *Nonlinear Dyn.* **92** 203
- [6] Liu R and Li J Z 2018 *Results Phys.* **11** 436
- [7] Li M M, Cheng L H, Wu J, Lai X J and Wang Y Y 2019 *Chin. Phys. B* **28** 120502
- [8] Lai X J, Cai X O and Zhang J F 2015 *Chin. Phys. B* **24** 070503
- [9] Chen W J, Ju Y, Liu C Y, Wang L K and Lu K Q 2018 *Chin. Phys. B* **27** 114216
- [10] Lan Z Z, Hu W Q and Guo B L 2019 *Appl. Math. Modell.* **73** 695
- [11] Lan Z Z and Su J J 2019 *Nonlinear Dyn.* **96** 2535
- [12] Longobucco M, Cimek J, Čurilla L, Pysz D, Buczyński R and Bugár I 2019 *Opt. Fiber Technol.* **51** 48
- [13] Soysouvanh S, Phongsanam P, Mitatha S, Ali J, Yupapin P, Amiri I S, Grattan K T V and Yoshida M 2019 *Microsyst. Technol.* **25** 431
- [14] Ghadi A and Sohrabfar S 2018 *IEEE Photon. Technol. Lett.* **30** 569
- [15] Laudyn U A, Piccardi A, Kwasny M, Karpierz M A and Assanto G 2018 *Opt. Lett.* **43** 2296
- [16] Banerjee A and Roy S 2018 *Phys. Rev. A* **98** 033806
- [17] Biswas A, Triki H, Zhou Q, Moshokoa S P, Ullah M Z and Belic M 2017 *Optik* **144** 357
- [18] Katti A 2018 *Appl. Phys. B* **124** 192
- [19] Katti A 2018 *Opt. Quantum Electron.* **50** 263
- [20] Cai X, Liu J S, Wang S L and Liu S X 2009 *Chin. Phys. B* **18** 1891
- [21] Shwetanshumala S and Konar S 2010 *Phys. Scr.* **82** 045404
- [22] Pu S Z, Chen M, Li Y J and Zhang L Y 2019 *Opt. Commun.* **450** 78
- [23] Saravanan M, Jagtap A D and Vasudeva M A S 2018 *Chaos Solitons Fractal.* **106** 220
- [24] Morin M, Duree G, Salamo G and Segev M 1995 *Opt. Lett.* **20** 2066
- [25] Lu K Q, Zhang M Z, Zhao W, Yang Y L, Yang Y, Zhang Y H, Liu X M, Zhang Y P and Song J P 2006 *Chin. Phys. Lett.* **23** 2770
- [26] Zheng C Z, Luo M Q, Lin G, Cui H and Luo A P 2017 *Opt. Commun.* **387** 95
- [27] Yan L F, Jin Q L, Zhang D and Zhang Y J 2011 *Opt. Commun.* **284** 1682
- [28] Yan L F, Wang H C and She W L 2006 *Acta Phys. Sin.* **55** 5257 (in Chinese)
- [29] Zhu W T, Cui H, Luo A P, Luo Z C and Xu W C 2016 *J. Opt. Soc. Am. B* **33** 2209
- [30] Ciattoni A, DelRe E, Marini A and Rizza C 2008 *Opt. Express* **16** 10867
- [31] Ciattoni A, DelRe E, Rizza C and Marini A 2008 *Opt. Lett.* **33** 2110
- [32] Cui H, Zhang B Z and She W L 2008 *J. Opt. Soc. Am. B* **25** 1756
- [33] She W L, Lee K K and Lee W K 1999 *Phys. Rev. Lett.* **83** 3182
- [34] She W L, Lee K K and Lee W K 2000 *Phys. Rev. Lett.* **85** 2498
- [35] Uzunov I M, Stoev V D and Tzoleva T I 1993 *Opt. Commun.* **97** 307